Journal of Statistics Applications & Probability
An International Journal

http://dx.doi.org/10.18576/jsap/130508

A Stochastic Model for HIV-TB Coinfection and Applications on Young Adults

Claris Shoko[1,*], *Wilford Molefe*[1], *and Pascal O. Bessong*[2]

[1] Statistics Department, Faculty of Social Sciences, University of Botswana, Gaborone, Botswana.
[2] HIV/AIDS & Global Health Research Programme, University of Venda, Thohoyandou, South Africa.

Received: 3 Apr. 2024, Revised: 20 May 2024, Accepted: 2 Aug. 2024.
Published online: 1 Sep. 2024.

Abstract: In this study, we investigate the progression of HIV/AIDS in patients with TB co-infection. Approximately one in three people living with HIV die due to TB. This hinders progress towards the achievement of the 2030 Sustainable Development Goal of ending the HIV and TB pandemic. We model the progression of HIV in patients with TB coinfection using multi-state modeling using data from HIV-TB co-infected young adults (15 to 34 years) from South Africa. HIV progression for this cohort is divided into 4 states (state 1: Undetectable viral load below 50 HIV RNA per mL; state-2: HIV ribonucleic acid (RNA) ranging from 50 to below 10 000 copies/mL; state-3: at least 10 000 HIV RNA copies/mL); and state-4: Death). Results from the analysis show that TB increases the log odds of an unsuppressed viral load. This is quite notable for patients in state 2 where the log-linear effect of having TB during treatment is approximately 5.776 for the transition from state-2 to state-3. At state-2 of HIV progression, the rate of virologic failure accelerates transitions to death from state-1 (3.806). This study is unique because it presents the interaction effects of viral load baseline and TB-coinfection as crucial in analyzing HIV progression among young adults.

Keywords: HIV-TB dynamics; Viral load suppression, Continuous-time homogeneous Markov model, young adults.

1. Introduction

Since 1985, infection with human immunodeficiency virus (HIV) has been known to be the risk factor behind the renewed epidemic of tuberculosis (TB). HIV infection is the most powerful risk factor predisposing to Mycobacterium TB (M.TB) infection and progression to active diseases which increases the risk of latent TB reactivation 20-fold [1,2] due to the impaired immune system. [3] also argued that within-host, Mycobacterium TB and HIV accelerate the deterioration of immunologic functions. TB is the leading cause of death among individuals infected with HIV with one in every four people living with HIV die due to TB [4]. MTB and HIV act in synergy, accelerating the decline of immunological (CD4+ T cell) functions a key marker of acquired immune deficiency syndrome (AIDS) progression and thus leading to the subsequent death of HIV-infected individuals.

Immune response to Mycobacteria tuberculosis

Tuberculosis is a disease caused by a bacterium called M. tuberculosis (M.TB). The transmission of the bacterium occurs by airborne spread of infectious droplets produced by a person with sputum smear-positive TB of the lung. Once infected the immune response takes 48 hours to 14 days to appear. After 24 hours of exposure, there is an intense increase in the population of both T cells and macrophages. Immune response to M.TB infection occurs in 2 ways: damage of the walls of the bacterium by the immune system cells and phagocytosis and digestion by macrophages. Bacteria are then transported by the dendritic cells to the closest lymph nodes where the host‘s adaptive immune response is mounted against infection.

However, from the primary infections, 90% do not progress to active tuberculosis as these are contained within the lungs in small granulomatous lesions that form at the site of infection known as granulomas. For these 90% of cases, the pathogen becomes dormant or latent. However, if the immune system is compromised, granuloma stability is thought to be breached thereby causing the M.TB to be released. 5% progress rapidly to active tuberculosis and die without treatment. The other 5% of the cases progress slowly over their lifetime.

During the initial stages of TB infection CD4+ and CD8+ T cells are activated and migrate to the site of infection where they interact with macrophages. CD4+ T cells help in activating and maintaining CD8+ effector and memory functions as well as the lysis of infected cells.

Immune response to HIV-1

Human immunodeficiency virus (HIV), the virus that causes acquired immunodeficiency syndrome (AIDS), is characterised by CD4 T cell depletion, CD8 T cell expansion, and chronic immune activation that leads to immune

*Corresponding author e-mail: shokoc@ub.ac.bw

dysfunction [5]. In 1988, Adleman suggested that the depletion in CD4 T cells might activate some homeostatic mechanism that increases their production. Catalfamo et al. [5] added that the proliferation of CD4 cells is not only driven by the depletion of CD4 cells but it is also driven by the viral load. However, proliferation of CD8 cells is driven by the external force, that is, the infection and in this particular case, HIV RNA levels. Hence, viral load is a significant driver of both CD4 and CD8 proliferation [6]. The CD8 T lymphocyte produces cytokines that limit the proliferation of HIV and also depletes the CD4 T cell that has HIV products [7,8].

HIV-1 is a virus that infects CD4+ T cells and macrophages that are critical to our immune system response thereby compromising the host's ability to control infection. Thus, HIV infection is characterised by a marked decline in the population of CD4+ T cells/mm^3 and a rise in viral load. The weakening of the immune system by HIV-1 makes people highly vulnerable to invasions by several infectious agents including M.TB.

Unlike M.TB which can reproduce independently, HIV-1 uses the CD4+ T cells to reproduce. HIV is an RNA-containing virus that uses the enzyme reverse transcriptase to produce a deoxyribonucleic acid (DNA) provirus that is inserted into the host cell's DNA. Once the cell is infected, it can be activated to proliferate and produce new virus particles. The production of new virus particles destroys the host cell leading to the eventual collapse of the immune system.

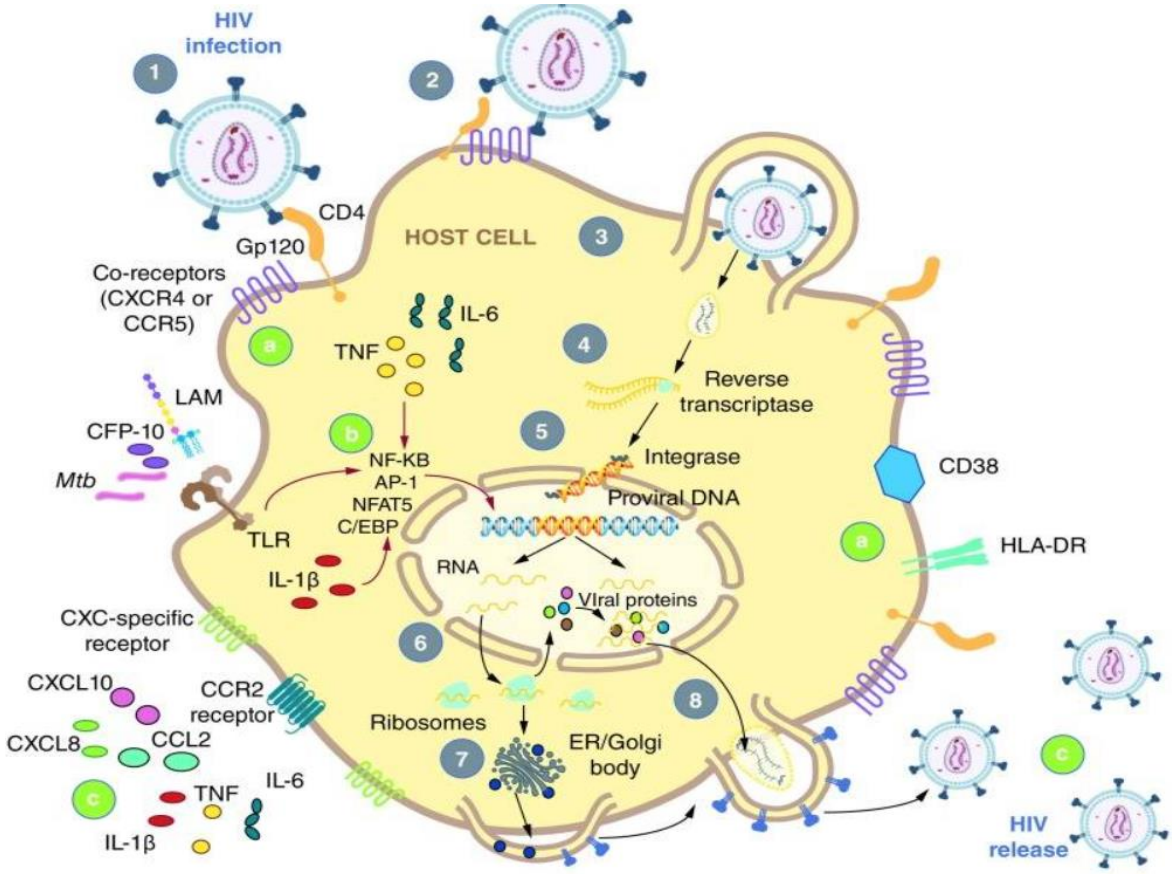

Fig. 1: HIV life cycle. Source Ndengane et al (2020) [9] https://www.ncbi.nlm.nih.gov/pmc/articles/PMC7132588/

2. Literature on modeling HIV/TB co-infection

The first attempt to understand the dynamics of co-infection with M. tuberculosis and HIV infection was by [10]. He created a mathematical model using ordinary differential equations (ODEs) to describe the interaction of HIV and TB with the immune system based on four populations that is $T(t)$ the armed CD4+ and CD8+ T cell populations at time t days, $M(t)$ the macrophage population, $V(t)$ the HIV population and $T_b(t)$ the M. tuberculosis population.

Bauer and others developed a mathematical model for an adaptive immune response in the lung, which considers relevant immune effectors such as macrophages, various sub-populations of T-cells, and key cytokines to predict which mechanisms are important to HIV infection due to the presence of M. tuberculosis. They used the deterministic approach. Their analysis

suggests that macrophages play an important role during co-infection and a decrease in macrophages coupled with a decrease in CD4 T-cell count increases viral load. They also discovered that these mechanisms are also coupled to lower recruitment of T-cells and macrophages, compromising protective immunity in the lung and eventually leading to TB reactivation

In 2009, Roeger et al [11] developed a TB/HIV model using a system of differential equations from a population. They divided the entire population into 8 subgroups namely, susceptible, latent with TB, infectious with TB, successfully treated with TB, HIV infections and TB latent, infectious with both TB and HIV, full-blown AIDS

In 2017, Tuite et al. [12] developed a stochastic agent-based model for TB transmission that captures the unique household and community structure. Their model includes the stages in the natural history of TB, that is, susceptible (for TB naïve individuals having never been infected with TB before and can be infected if they come in contact with individuals with active TB), latent TB infection (individuals recently infected with TB), active TB (small proportion proceed to develop active pulmonary TB within a period of 5 years) and re-susceptible (individuals who have been successfully treated for TB or who successfully cleared their TB without receiving treatment transition to the re-susceptible compartment).

Most of the studies cited above considered the dynamics of HIV/TB co-infection at population level. A lot more studies also considered the dynamics of the diseases spread at the population level [13-15]. However, understanding the dynamics of the spread of infectious diseases brings possibilities of its control [16]. Only a few studies considered the pathogenesis within an infected individual [10-18]. These studies used the deterministic approach to mathematical modeling except for the study by Kirschmer, 1999 [10].

Mathematical models often need to incorporate intrinsic stochasticity because the size of the population of infected hosts is random and integer-valued has many important consequences. According to Tuckwell, the stochastic approach provides a more accurate quantitative basis for evaluating the efficacy of treatment in infected host cells since it has the following effects:

- Generation and fluctuation in the rate of appearance of new host cells,
- Contacts between viruses and the host cells and the random attachment,
- Transition to active infected cells,
- Time for the emergence of new virions,
- Number of new virions emerging from a host cell,
- Death of infected and uninfected host cells and virions,
- Appearance and action of immune system components which assist in the removal of virions.

Although the stochastic approach to disease modelling has more advantages compared to the deterministic model, any stochastic epidemic model has a deterministic counterpart which is obtained by setting the deterministic population increments equal to the expected values of the conditional increments in the stochastic model [16].

HIV-Tuberculosis interaction with the immune system

Formulation of the model is based on the assumption that at time t=0, an individual becomes infected with HIV. The main target of the virus is the CD4 T cell (T_4). Once the virus penetrates this cell it becomes HIV-infected (T_{4v}) the natural immune system responds by triggering the production of CD8 T cells (T_8) to produce virus-specific T cells (T_{8v}). These cells are cytotoxic; hence they act as predators that help eliminate the HIV-infected CD4 T cells (T_{4v}). The CD4 T cells that escape killing by the cytotoxic cells become productively infective and produce millions of new HIV particles (V) and these CD4 cells are destroyed in the process. The new viruses target more CD4 T cells, thereby reducing the population of CD4 cells. The process goes on and on. This continuous depletion in CD4 cells compromises the immune system.

As the immune system is compromised, it leads to activation of the latent M. tuberculosis (MTB) leading to HIV/TB co-infection. The immune system responds to M. tuberculosis by producing macrophage-specific T cells (T_{8m}) that damage the walls of M. tuberculosis and also macrophages (M) are produced that attack the bacteria by engulfing it (the process is called phagocytosis). The macrophages (M) then hold the M. tuberculosis by forming granulomas. Some of the macrophages can also help in engulfing HIV. Thus, we can have a population of M. tuberculosis-infected macrophages ($M_{m)}$, HIV-infected macrophages (M_v), or even HIV/TB co-infected macrophages (M_c) introduced into the system. These infected macrophages produce new populations of HIV particles into the system but at a slower rate compared to the viruses produced by the infected CD4 T cells. They also produce new particles of M. tuberculosis into the system. Besides the production of M. tuberculosis by the macrophages, there is also a natural splitting of M. tuberculosis leading to the increase in the population of M. tuberculosis within the system.

Figure 2 below is a diagram that represents possible interactions of HIV and M. tuberculosis with the immune system in the absence of antiretroviral therapy.

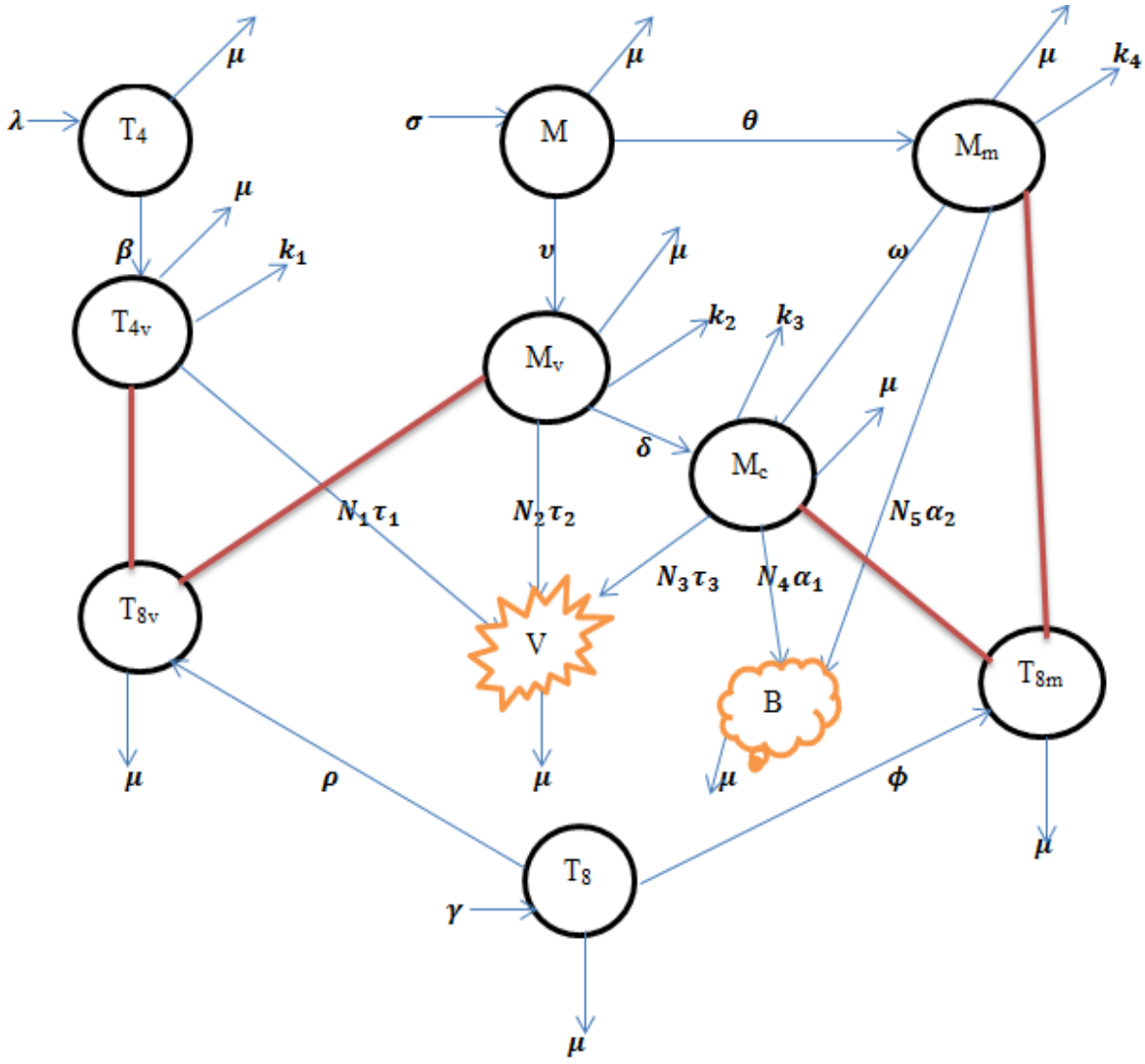

Fig. 2: HIV/TB Dynamics

Figure 2 shows that our model divides the in-vivo immune response to M. tuberculosis and HIV in the absence of ART into 11 mutually exclusive components defined in Table 1 below

Table 1: Description of model variables

Variables	Description
T_4	Susceptible CD4 T-cells
T_{4v}	CD4 T-cells infected by HIV
T_{8v}	HIV-specific CD8 T-cell
M	Macrophages
M_v	Macrophages infected by HIV
M_m	Macrophages infected by M. tuberculosis
M_c	Macrophages co-infected by both HIV and M. tuberculosis
T_8	CD8 T-cells
T_{8m}	Macrophage-specific CD8 T-cell
V	Virus particles
B	M. tuberculosis particles

Thus, at time t the total population ($N(t)$) is given by

$$N(t) = \mathrm{T}_4(t) + \mathrm{T}_{4v}(t) + \mathrm{T}_{8v}(t) + M(t) + \mathrm{M}_v(t) + \mathrm{M}_m(t) + \mathrm{M}_c(t) + \mathrm{T}_8(t) + \mathrm{T}_{8m}(t) + V(t) + B(t) \quad (1)$$

HIV infected cells are recruited into the pool at a rate of:

$$\lambda_v(t) = \frac{\beta_v}{N(t)}(\mathrm{T}_{4v}(t) + \mathrm{T}_{8v}(t) + \mathrm{M}_v(t) + \mathrm{M}_c(t) + V(t)) \quad (2)$$

where β_v is the effective contact rate of HIV infection.

M. tuberculosis-infected cells are recruited into the pool at a rate of:

$$\lambda_m(t) = \frac{\beta_m}{N(t)}(\mathrm{T}_{8m}(t) + \mathrm{M}_m(t) + \mathrm{M}_c(t) + B(t)) \quad (3)$$

where β_m is the effective contact rate of TB infection.

The set of parameters in our model are defined below:

Table 2: Description of model parameters

Parameters	Description
λ	Rate of production of CD4 T-cells from the source
σ	Rate at which macrophages are recruited from the source
γ	Rate at which CD8 T-cells are recruited from the source
μ	Natural death rate of cells
β	Rate at which CD4 T-cells become infected by HIV
α_i	Rate of production of M. tuberculosis by macrophages
k_i	Rate at which infected CD4 T-cells and macrophages are cleared by CD8 T-cells
N_i	Number of virus particles or bacterium produced by cells or macrophages that survived attack by CD8 T-cells
ν	Rate at which macrophages become infected by HIV
θ	Rate at which macrophages are infected by M. tuberculosis
ω	Rate at which M. tuberculosis infected macrophages are co-infected by HIV
δ	Rate at which virus infected macrophages become co-infected by M. tuberculosis
τ_i	Rate at which viruses are produced by infected CD4 T-cells and macrophages
ϕ	Rate at which M. tuberculosis-specific CD8 T-cells are produced
ρ	Rate at which HIV-specific CD8 T-cells are produced

The model in Figure 1 can be represented by the following system of differential equations:

$$\frac{dT_4}{dt} = \lambda - \mu T_4 - \beta V T_4 \quad (4)$$

$$\frac{dT_{4v}}{dt} = \beta V T_4 - k_1 T_{8v} T_{4v} - \mu T_{4v} \quad (5)$$

$$\frac{dT_{8v}}{dt} = \rho T_8 - \mu T_{8v} \quad (6)$$

$$\frac{dT_8}{dt} = \gamma - \phi T_8 M_m - \rho T_8 T_{4v} - \mu T_8 \quad (7)$$

$$\frac{dT_{8m}}{dt} = \phi T_8 M_m - \mu T_{8m} \quad (8)$$

$$\frac{dM}{dt} = \sigma - \mu M - \upsilon V M - \theta B M \quad (9)$$

$$\frac{dM_v}{dt} = \upsilon V M - k_2 T_{8v} M_v - \delta B M_v - \mu M_v \quad (10)$$

$$\frac{dM_m}{dt} = \theta B M - k_4 T_{8m} M_m - \omega V M_m - \mu M_m \quad (11)$$

$$\frac{dM_c}{dt} = \delta B M_v + \omega V M_m - k_3 T_{8m} M_c - k_5 T_{8v} M_c - \mu M_c \quad (12)$$

$$\frac{dV}{dt} = \tau_2 M_v + \tau_3 M_c + \tau_1 T_{4v} - \mu V \quad (13)$$

$$\frac{dB}{dt} = \alpha_1 M_c + \alpha_2 M_m - \mu B \quad (14)$$

The differential equations are subject to the initial conditions given by:

Table 3: Initial conditions for the differential equation

$T_4(0) = T_{40} \geq 0$	$T_{4v}(0) = T_{4v0} \geq 0$	$T_{8v}(0) = T_{8v0} \geq 0$	$M(0) = M_0 \geq 0$
$M_v(0) = M_{v0} \geq 0$	$M_m(0) = M_{m0} \geq 0$	$M_c(0) = M_{c0} \geq 0$	$T_8(0) = T_{80} \geq 0$
$T_{8m}(0) = T_{8m0} = 0$	$V(0) = V_0 \geq 0$	$B(0) = B_0 \geq 0$	

Our model differs from the human population models in that it caters for the interaction between cells and pathogenesis invivo. The solutions to the differential equations are presented in the Appendix section. For example, in the first differential equation, HIV (V) interacts with the susceptible CD4 cell (T_4) resulting in the transition of T_4 to an HIV-infected CD4 cell (T_{4v}). Hence the inclusion of the term $\beta V T_4$, defines the binding of the CD4 cell with HIV particles. With human population models, contact with HIV-infected individuals results in a transition from susceptible to HIV infected without a permanent binding of the susceptible and the infected.

In the next section, we present an analysis of HIV-TB coinfection using a cohort of young adults under treatment follow-up for 5 years in South Africa.

3. Materials and Methods

Aim, Design and Study Setting

A retrospective study using secondary data of a cohort that was on treatment follow-up in Bela-Bela, South Africa. The study area and sample collection Bela-Bela clinic was selected as the study site for the collection of samples. This clinic services a large population from different areas of Limpopo Province, South Africa. This clinic is situated in an area that is recognized as a resting place for travelers. Samie et al. [19] presents more information on the aim, design, and study setting. They also give a description of the materials used. This study is based on secondary data in which all the names of participants were stripped off before getting the data set. This study considers a sample of all young adult participants in the age group 15 to 34 years. The next subsection describes the young adults considered in this study.

Descriptive data

Patients were put on combination antiretroviral therapy (cART) at time t=0. A cohort of 97 HIV-TB co-infected young adults (15 to 34 years) was considered for analysis. Young adults constitute the most sexually active age group compared to all the other age groups. At enrolment, the patients had a minimum viral load baseline of 122, a maximum of 419662 and an average of 81609 HIV RNA/mL. The minimum CD4 baseline was 10, a maximum of 662, and an average of 169 cells/mL. The average age of patients was 31 years of enrolment. The patients were monitored after 3 months (0.25 years) of cART and after that in follow-up intervals of 6 months (0.5 years). Follow-up was done for a maximum of 5 years but due to some deaths and withdrawal cases associated with the data, the average follow-up time for each patient in this study is 3.5 years. In the first 1.5 years of treatment, the majority of young adults were on D4T-3TC-EFV (57%) and D4T-3TC-NVP (27%) treatment combinations, and from 2 years onwards most patients were on AZT-3TC-EFV (63%) and AZT-3TC-NVP (19%) treatment combinations. D4T (Stavudine), 3TC (Lamivudine), EFV (Efavirenz), NVP (Nevirapine), AZT (Zidovudine) are antiretroviral medicines used to treat HIV/AIDS.

At follow-up times, the effectiveness of cART was assessed by changes in the HIV viral load level. Attainment of a suppressed viral load below the level of detection within the first 6 months indicated good adherence to treatment and effectiveness of cART. In this study, the level of detection is 50 viral RNA copies/mL and above.

The viral load levels during treatment for each individual is classified into states based on the severity of the patient's condition as follows:

$$VLS = \begin{cases} State\ 1,\ if\ VL < 50 \\ State\ 2,\ if 50 \leq VL < 10\,000 \\ State\ 3,\ if\ VL \geq 10\,000 \\ State\ 4,\ if\ dead \end{cases} \quad (15)$$

States $i = 1,2,3$ are the live/transient states and states 4 are the absorbing states. Transitions from state i to $i + k$, where $k > 0$ represents disease progression to worse states and transitions and $k < 0$, represents disease progression to better states. The log-linear effects of developing TB during the course of treatment (TBEN), having TB before enrolment into ART (TBBF) , having virologic failure (VF), and gender on HIV progression is analysed. The variables are coded as shown below.

VF = $\begin{cases} 1,\ Yes \\ 0,\ No \end{cases}$, TBEN = $\begin{cases} 1,\ Yes \\ 0,\ No \end{cases}$, Gender = $\begin{cases} 1,\ male \\ 0, female \end{cases}$, TBBF = $\begin{cases} 1,\ Yes \\ 0,\ No \end{cases}$

Statistical Analysis

A time-homogeneous Markov modeling approach to Stochastic processes is used to analyse the invivo dynamics of HIV-TB coinfection for patients under treatment follow-up. This is done using the "MSM" package for multistate modeling in R. The Markov model is made up of the states, transition probabilities, and initial transitions. Thus, a Markov model is a type of stochastic or random process. This makes it more intuitive because real life is not deterministic but stochastic, in particular the invivo dynamics of HIV-TB coinfection. Stochastic processes are also good at handling the effects of covariates. In this study, the states are defined based on viral load levels as shown in equation (16). The Markov model can be written as a log-linear model as shown below;

$$ln\ q_{ijh} = \beta_{ij0} + \beta_{ij1} TBB4_h + \beta_{ij2} TBEN_h + \beta_{ij3} VF_h + \beta_{ij4} Gender_h,\ \ i \neq j \quad (16)$$

where $\exp\{\beta_{ij0}\} = q_{ij}^{(0)}$ the baseline transition rates for patients in which the covariates are not mentioned and β_{ijs} for s=1,2,3,4 represents the log-linear effects of covariate *s* on the transition intensities.

Assessment of the fitted model

Selection of the best number of states to describe the transition is done by first considering the 7-state model, 6-state, 5-state, and 4-state models. The number of states with a positive definite Hessian matrix is considered for further analysis. The performance of the fitted models is further assessed using the likelihood ratio test. The model with the highest log-likelihood is considered as the best model. The Akaike Information Criteria (AIC) for each model are also computed. The most accurate model yields the lowest AIC. For each of the fitted parameters, the confidence intervals are presented and used to test the following hypothesis at $\alpha = 5\%$:

$H_0: \beta_{ijs} = 0$: The mentioned variable does not have any significant log-linear effect,

$H_1: \beta_{ijs} \neq 0$: The variable mentioned has a significant log-linear effect

The 7-state model that we started with is defined as follows:

$$\boldsymbol{VLS = \begin{cases} State\ 1,\ if\ VL < 50 \\ State\ 2,\ if 50 \leq VL < 1\,000 \\ State\ 3,\ if 1\,000 \leq VL < 10\,000 \\ State\ 4,\ if 10\,000 \leq VL < 100\,000 \\ State\ 5,\ if 100\,000 \leq VL < 500\,000 \\ State\ 6,\ if\ VL \geq 500\,000 \\ State\ 7,\ if\ dead \end{cases}} \quad (17)$$

Where state 1 represents the undetectable viral load state and state 2 represents the suppressed viral load states. These two states are the most important as they represent treatment efficacy. Further division of states helps in determining any possibilities of viral rebound at different viral load levels.

4. Results and Discussions

Descriptive statistics

At t=0 there were 0 patients with undetectable viral load (state 1); 12 patients with a viral load between 50 and 10 000 (state **2)**; and 85 (87.63%) patients with a viral load above 10 000 copies/ml; and no deaths. Initially, the study started with 77 women and 20 men. 10 women and 2 men were in state 2 and 67 women and 18 men were in state 3. Thus, all $t = 0$ all the patients were alive.

Fitting a Markov Model for the 15-to-34-year age group

In this section, we fit a continuous-time homogeneous model to analyse the progression of HIV/ADS among young adults, 15 to 34 years, who developed TB during treatment follow-up. For this cohort, there were no patients with undetectable viral loads at treatment initiation. The analysis is done using the "msm" package for R developed by Christopher Jackson [20]. We started by fitting a time-homogeneous model without covariates to assess the number of transitions to each state, the transition rate matrix, the probability matrix, and the probability of each state being next. To select the best number of states we started with a 7-state model and reduced the number of states until a positive definite Hessian matrix was obtained. The 4-state Markov model had a positive definite Hessian matrix, and the parameters of the model are presented in Table 4.

Table 4: Transition matrices and corresponding 95% Confidence Interval

From\To	State 1	State 2	State 3	State 4
	State matrix			
State 1	363	26	0	10
State 2	59	29	9	12
State 3	36	52	14	4
	Intensity matrix			
State 1	-0.305 (-0.441,-0.210)	0.262 (0.171,0. 403)	0	0.042 (0.018, 0.101)
State 2	2.813 (2.201, 3.596)	-6.303 (-9.480,-4.191)	3.078 (1.334, 7.101)	0.4118 (0.239, 0.710)
State 3	0	15.23 (7.722, 30.020)	-15.230 (-30.020,-7.722)	0.000027 (3.719e-99, 1.968e+89)
State 4	0	0	0	0
	Probability of each state being next			
State 1	0	0.862 (0.691,0.945)	0	0.138 (0.055,0.309)
State 2	0.446 (0.254,0.626)	0	0.488 (0.284,0.713)	0.065 (0.031,0.118)
State 3	0	1.000 (5.286e-87,1.000)	0	1.777e-06 (3.064e-105,1.00)
State 4	0	0	0	0
-2 * log-likelihood: 808.965; AIC= 822.965				
$State\ 1,\ if\ VL < 50, State\ 2,\ if 50 \leq VL < 10\ 000, State\ 3,\ if\ VL \geq 10\ 000, State\ 4,\ if\ dead$				

The results from Table 4 show that although there were no patients in state 1, which is the undetectable viral load state, at t=0, during treatment there were more transitions into state 1 followed by state 2 (HIV RNA copies between 50 and 10 000). This shows the efficacy of the treatment. A further analysis of transitions is done using the intensity matrix. Results from the intensity matrix show that state 3 (with HIV RNA copies greater than 10 000), which initially had the greatest percentage of patients (87.6%), transition rates to state 2 were higher than transition rates to state 4 (which represents death, the absorbing state). However, from state 2 transition rate to state 3 is higher than the transition rate to state 1. This is a cause of concern since antiretroviral therapy is expected to cause viral suppression within the first three months of uptake. Given that a patient is in state 2, the probability that s/he jumps to state 3 is higher than the probability that s/he jumps to state 1, a further confirmation of the results presented by the transition rate matrix. In Table 5 we present the expected total time spent in each state and the mean sojourn times. The expected holding time or mean sojourn times together with the total time spent in each state or jump chain give the full description of a time-homogeneous Markov model. The mean sojourn time represents the average time spent in each state during the follow-up period.

Table 5: Mean sojourn times

	Total time spent in each state (Years)	Mean sojourn times (95% CI)
State 1	13.22	3.28 (2.27, 4.75)
State 2	1.06	0.16 (0.11, 0.24)
State 3	0.22	0.06 (0.03, 0.13)
state 4	Inf	
$State\ 1,\ if\ VL < 50, State\ 2,\ if 50 \leq VL < 10\ 000, State\ 3,\ if\ VL \geq 10\ 000, State\ 4,\ if\ dead$		

Results in Table 5 show that for the five–year follow-up period the expected holding time in the undetectable viral load state is 3.28 years and the unsuppressed viral load state has the least. Forecasts made from this study show that once the viral load is reached a patient is expected to spend approximately 13 years before being absorbed into the death state. Although based on CD4 cell count states, the findings from the study by Shoko and Chikobvu [21] also confirm that once a patient is in the best state, s/he is likely to spend more time in that state.

State 3 has the least expected total time. In Table 6 we present the log-linear effects and the corresponding confidence intervals of developing TB during treatment, being diagnosed of TB at enrolment, viral load baseline, having virologic failure, and gender with male being the reference category. When the model was fitted with no interaction effects, the Hessian matrix was not positively definite. Several interactions between the variables were considered and finally, the interaction of the viral load baseline and developing TB during treatment resulted in a positive Hessian matrix implying convergence. The risk ratios are presented together with the confidence intervals. The exclusion of one (1) in the confidence interval implies that the effect is significant.

Table 6: Log-linear effects of having TB before ART initiation, developing TB after treatment initiation (TBEN), gender, and virologic failure

From\To	State 1	State 2	State 3	State 4
	Viral Load Baseline of at least 10 000 copies/mL			
State 1	0	0.47(0.082,2.74)	0	1.40 (0.02, 104.38)
State 2	**0.35(0.13,0.93)***	0	587.57 (e^(-20.401),e^(33.160))	**0.064(0.0045, 0.92)***
State 3	0	6.49(1.27,e^(14.79))	0	1.03 (e^{-214.742},e^{214.79})
State 4	0	0	0	0
	TB during the course of treatment			
State 1	0	1.10 (0.164, 7.41)	0	0.0054 (e^{-33.304},e^{22.874})
State 2	0.52 (0.15, 1.87)	0	322.47(e^{-21.035},e^{32.59})	0.41 (0.038, 4.42)
State 3	0	0.63 (0.077, 5.08)	0	0.998 (e^{-230.13},e^{230.13})
State 4	0	0	0	0
	Gender (Male=1)			
State 1	0	1.81 (0.60, 5.43)	0	0.0003(e^{-53.34}, e^{37.018})
State 2	**2.13 (1.10, 4.10)***	0	0.092 (e^{-103.5}, e^{98.72})	0.002 (e^{-46.95}, e^{34.263})
State 3	0	411.58 (e^{-42.26}, e^{54.29})	0	2.82 (e^{-1291}, e^{1292.65})
State 4	0	0	0	0
	TB at enrolment into ART			
State 1	0	**0.21 (0.043, 0.99)***	0	**0.11 (0.032, 0.390)***
State 2	1.94 (0.21, 1.24)	0	0.82 (0.027, 24.95)	82.60 (e^{-37.065}, e^{45.893})
State 3	0	0.87 (0.052, 14.31)	0	1.15 (e^{-144.66},e^{144.94})
State 4	0	0	0	0
	Virologic Failure			
State 1	0	15.36 (1.097, 215.08)	0	44.97 (2.25, 898.75)
State 2	0.53 (0.105, 2.71)	0	1.53 (0.107, 21.80)	0.04 (e^{-50.69},e^{44.19})
State 3	0	0.39 (0.031, 5.05)	0	0.77 (e^{-109.8},e^{109.31})
State 4	0	0	0	0
	Interaction Viral load baseline above 10 000copies/mL and TB during the course of treatment			
State 1	0	0.85 (0.09, 8.21)	0	70.74 (e^{-23.867}, e^{32.385})
State 2	2.94 (0.69, 12.59)	0	0.07 (e^{-80.81},e^{75.478})	0.12 (e^{-53.56}, e^{49.38})
State 3	0	103.03 (e^{-68.643}, e^{77.91})	0	2.07 (e^{-354.75},e^{356.20})
State 4	0	0	0	0
	-2 * log-likelihood: 651.615; AIC= 749.615			
	$State\ 1,\ if\ VL < 50, State\ 2,\ if 50 \leq VL < 10\,000, State\ 3,\ if\ VL \geq 10\,000,$ $State\ 4,\ if\ dead$			

Inclusion of the covariates together with the interaction effect between the VLBL and TB during the treatment results in the reduction of the -2*log-likelihood and AIC from 808.965 to 651.615 and 822.965 to 749.615 respectively. The model that includes the effect of TB at enrolment, TB during treatment, gender, virologic failure, and in particular the interaction effects of TB and Viral load baseline was the best model for this particular cohort. A study by Karaca-Mandic et al. [22] emphasised the importance of including interaction effects in statistical models. This study confirms the importance of the inclusion of the interaction effects since this resulted in the reduction of the AIC and an increase in the log-likelihood ratio. This study further shows reduced risks of transitions to better viral load states and increased risk of transitions to worst viral load states for patients with viral load baseline above 10,000 copies/ml. This calls for the need by the Public Health sector to establish mobile clinics and encourage voluntary HIV and TB testing as well as educate them on the importance of treatment adherence.

As presented in Table 6, young adults, diagnosed with TB before initiation of cART had a 79% reduced risk of viral suppression compared to those with no TB. Developing TB during treatment results in increased transitions from viral load between 50 and 10

000 (state 2) to a viral load level greater than 10 000 (state 3). However, after TB treatment and immunological response, an increase in transition from state 3 to state 2 is observed. Antiretroviral therapy coupled with the immunological response MTB helps to clear the HIV RNA copies in the blood plasma as presented in Figure 2. Among these HIV-TB coinfected patients, the effect of virologic failure increases transition from state 2 to state 3 by 52%. For the HIV-TB co-infected young adults, men are 2.13 times more likely to experience viral suppression compared to their female counterparts.

Results from Table 6 show that if patients develop TB during the course of ART there is increased risk of viral load rebound from a viral load level between 50 and 10 000 copies/mL to a viral load level above 10 000 copies/mL. Results from the study by Moreto et al. [23] show an amplified progression of HIV to AIDS due to M. Tuberculosis are in congruent with this study. The log-linear effect of virological failure between these states is approximately 3.2. These results concur with the findings from a study that was carried out in Ethiopia by Getaneh et al. [24]. Although they used a different approach in their analysis, their results showed that for adults the odds ratio of unsuppressed viral load among HIV-TB patients is 2.46 compared with patients with HIV only. The effect of having TB before ART is also unfavourable. Findings from Shoko et al. [25], based on a cohort of all age groups (infants, children, adolescents, adults, and the elderly) also show that the development of TB contributes significantly to unsuppressed viral load. Another study carried out using a prospective cohort study in KwaZulu Natal in South Africa also confirms that an increase in viral load is associated with TB co-infected patients [26]. This calls for the need to introduce TB preventive measures among the HIV infected cohorts. These measures can be in the form of TB vaccines for individuals with latent TB. The other alternative can be introducing treatment partners who closely monitor treatment uptake by HIV infected individuals for a sustained viral suppression. Once the viral load remains suppressed and the immune system is strong, the risk of TB infection is reduced.

For the HIV-TB co-infected young adults, men have higher log-linear effects of viral suppression compared to the females. The reasons for this are not quite clear but with this cohort, 79.4% were females which might make it difficult to compare the progressions by gender. Other researchers cite the socioeconomic status of women as the potential reason. Women are usually disadvantaged in terms of economic resources and social positions [27]. Treatment for HIV-TB co-infected individuals requires a good and balanced diet for them to push along. Thus, in addition to treatment, these individuals need support in terms of food in order for them to fight the combined burden of HIV and TB.

Figure 3 presents the prevalence plots for each state at each follow-up time. This helps to give a visual perception of the transitions for the HIV-TB co-infected young adults.

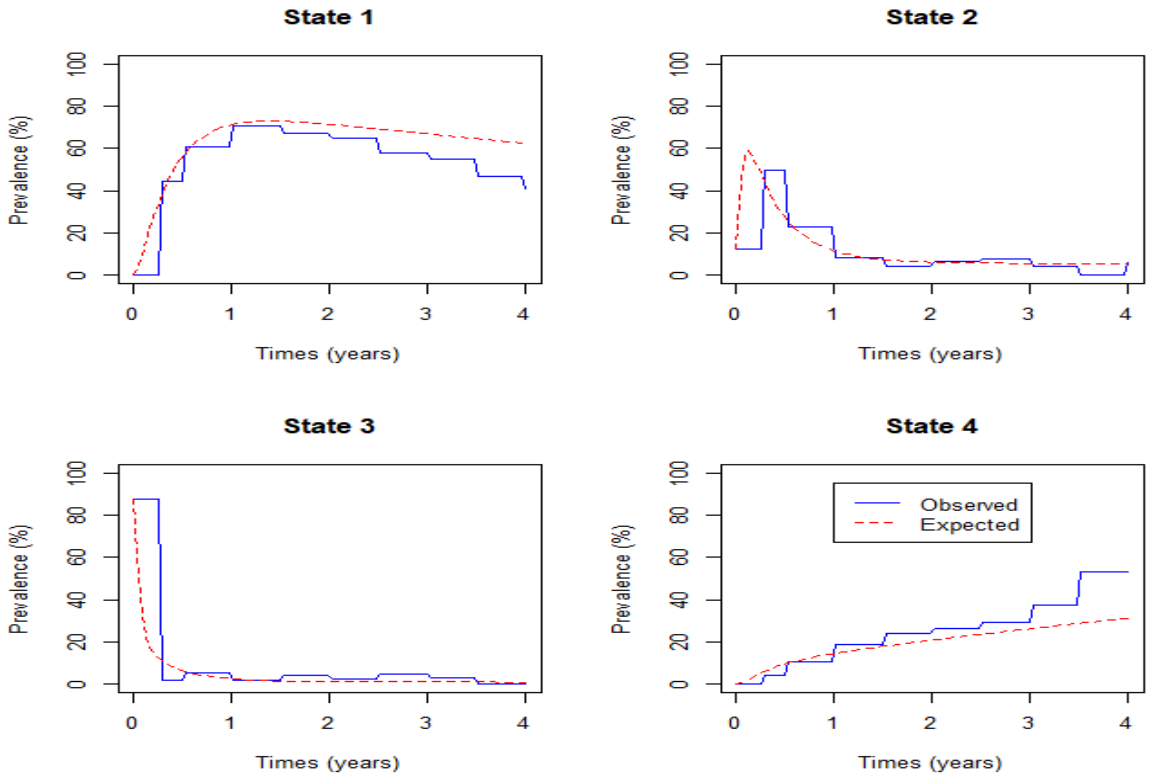

Fig. 3: Prevalence plots for each state

Figure 3 shows that at t=0, there were no young adults with undetectable viral load (below 50 copies/mL), less than 15% had viral load between 50 and 10 000 copies/mL, more than 85% of the young adults had viral load greater than 10 000 copies/mL, and no deaths. However, after 3 months an influx of patients into the undetectable viral load state is observed, and a sharp drop of the percentage of young adults in state 3. A rise in the percentage of patients into state 2 is also observed for the same period though it is not as high as that of state 1. Although there were no young adults with undetectable viral loads at enrolment, after half a year of treatment follow-up there were more patients with undetectable viral loads compared with the other states. A study by Dessie [28], though it is based on CD4 cell count states, shows higher rates of transitions to better states than to worst states as a result of treatment efficacy.

5. Conclusion

The combined burden of HIV and TB may impede efforts to implement the End TB Strategy [29] and the Declaration of the UN General Assembly high-level meeting on the fight against TB [30]. Comprehensive treatment plans, diagnostic procedures, and preventative measures are required for HIV-TB coinfection. Furthermore, to ensure the highest possible success rates, gradual reduction, and eventual cessation of the burden caused by TB and HIV, healthcare institutions, practitioners working with individuals living with HIV and TB, and civil society should work toward closer collaboration and full integration of services. These efforts should concentrate on strengthening the health system, governance, human resources, monitoring, and evaluation, as well as, when applicable, addressing institutional bias and social stigma and institutional bias—so that the burden caused by TB/HIV coinfection can be gradually reduced and eventually eliminated, all while ensuring the best success rates possible. These initiatives will enhance the lives of those afflicted by these illnesses and lead to better public health outcomes.

6. Limitations of the study

The sample size used for this study was small. This has led to the decision of redefining the suppressed viral load state as $[50, 10\ 000)$. Thus, bypassing the current WHO limits of viral load suppression. The other limitation is on the use of the multistate modeling approach. The approach could not account for the nonlinear effect of age resulting in the age variables being categorized. Its present findings should also be seen in light of the current recommended standard first-line treatment regimen which is Tenofovir-Lamivudine-Dolutegravir.

Abbreviations

AIDS	Acquired immunodeficiency syndrome
DNA	Deoxyribonucleic acid
HIV	Human immunodeficiency virus
MSM	Multi-state modelling
M.TB	Mycobacterial Tuberculosis
RNA	Ribonucleic acid
TB	Tuberculosis
TBBF	TB before ART
TBEN	TB after enrolment
VF	Virologic failure
WHO	World Health Organisation

7. Declarations

- Ethics approval and consent to participate

The procedures used in this study were as approved by the Research Ethics Committee of the University of Venda, South Africa (Protocol number SMNS/13/MBY/01/0625), in accordance with the 1964 Helsinki declaration and its subsequent amendments. Additionally, permission to access health facilities was obtained from the Limpopo Provincial Department of Health, South Africa, and the collaborating health facilities. Informed consent was obtained from study participants prior to their involvement; and data obtained was stripped of personal identifiers to ensure the confidentiality of the participants.

- Acknowledgements

The authors would like to acknowledge the University of Botswana and the University of Venda for giving us time to do this research. Research reported in this publication received partial support from the South African Medical Research Council (SAMRC) and National Research Foundation of South Africa (NRF) (Grant No: 141916). The content and findings reported are the sole deduction, view and responsibility of the researchers and do not reflect the official position and sentiments of the SAMRC, NRF or affiliations of the authors.

References

[1] Moreno R, Ravasi G, Avedillo P, Lopez R. Tuberculosis and HIV coinfection and related collaborative activities in Latin America the Caribbean. Rev Panam Salud Publica. 2020;44:e43. https://doi.org/10.26633/RPSP.2020.43 .

[2] Pawlowski A, Jansson M, Sköld M, Rottenberg ME, Källenius G. Tuberculosis and HIV co-infection. PLoS Pathog. 2012 Feb;8(2):e1002464. doi: 10.1371/journal.ppat.1002464. Epub 2012 Feb 16. PMID: 22363214; PMCID: PMC3280977.

[3] Ganesan, Kavitha; Mwesigwa, Ronald; Dear, Nicole; Esber, Allahna L.; Reed, Domonique; Kibuuka, Hannah; Iroezindu, Michael; Bahemana, Emmanuel; Owuoth, John; Singoei, Valentine; Maswai, Jonah; Parikh, Ajay P.; Crowell, Trevor A. MD; Ake, Julie A.; Polyak, Christina S.; Shah, Neha; Cavanaugh, Joseph S.; . Epidemiology of Tuberculosis Among People Living With HIV in the African Cohort Study From 2013 to 2021. JAIDS Journal of Acquired Immune Deficiency Syndromes 92(5):p 359-369, April 15, 2023. | DOI: 10.1097/QAI.0000000000003152.

[4] Ngari MM, Rashid MA, Sanga D, Mathenge H, Agoro O, Mberia JK, Katana GG, Vaillant M, Abdullahi OA. Burden of HIV and treatment outcomes among TB patients in rural Kenya: a 9-year longitudinal study. BMC Infect Dis. 2023 May 30;23(1):362. doi: 10.1186/s12879-023-08347-0. PMID: 37254064; PMCID: PMC10227789.

[5] Catalfamo M., Wilhelm C., Tcheung L., Proschan M., Friesen T., Park J., Adelsberger J., Baseler M., Maldarelli F., Davey R., Roby G., Rehm C., and Lane C.; CD4 and CD8 T Cell Immune Activation during Chronic HIV Infection: Roles of Homeostasis, HIV, Type I IFN, and IL-7; \emph{J Immunol 2011}; 186:2106-2116; Accessed on: http://www.jimmunol.org/content/186/4/21006.

[6] Hraba T, Dolezal J. Mathematical modelling of HIV infection therapy. Int J Immunopharmacol 1996;17:523-6.

[7] Ho D, Neumann AU, Perelson AS, Chen W, Leonard JM, Markowitz M, et al. Rapid turnover of plasma virions and CD4 lymphocytes in HIV-1 infection. Nature 1995;373:123-6.

[8] Wei X., Ghosh S.K., Taylor M.E., Johnson V.A., Emini E.A., Deutsch P., \textit{et al.}. Viral dynamics in human immunodeficiency virus type 1 infection. Nature 1995;373:117-22.

[9] Waters R, Ndengane M, Abrahams MR, Diedrich CR, Wilkinson RJ, Coussens AK. The *Mtb*-HIV syndemic interaction: why treating *M. tuberculosis* infection may be crucial for HIV-1 eradication. Future Virol. 2020 Feb;15(2):101-125. doi: 10.2217/fvl-2019-0069. PMID: 32273900; PMCID: PMC7132588.

[10] Kirschner D. Dynamics of co-infection with M. Tuberculosis and HIV-1. Theor Popul Biol. 1999 Feb;55(1):94-109. doi: 10.1006/tpbi.1998.1382. PMID: 9925811.

[11] Roeger LI, Feng Z, Castillo-Chavez C. Modeling TB and HIV co-infections. Math Biosci Eng. 2009 Oct;6(4):815-37. doi: 10.3934/mbe.2009.6.815. PMID: 19835430.

[12] Tuite AR, Gallant V, Randell E, Bourgeois AC, Greer AL. Stochastic agent-based modeling of tuberculosis in Canadian Indigenous communities. BMC Public Health. 2017 Jan 13;17(1):73. doi: 10.1186/s12889-016-3996-7. PMID: 28086846; PMCID: PMC5237134.

[13] Shah SA, Altaf A, Mujeeb SA, and Memon A (2004). An outbreak of HIV infection among injection drug users in a small town in Pakistan: potential for national implications. International Journal of STD & AIDS, 15(3):209-210.

[14] Bolarin G., Omatola I. U., A Mathematical Analysis of HIV/TB Co-Infection Model, *Applied Mathematics*, Vol. 6 No. 4, 2016, pp. 65-72. doi: 10.5923/j.am.20160604.01.

[15] Bacaër N, Ouifki R, Pretorius C, Wood R, Williams B. Modeling the joint epidemics of TB and HIV in a South African township. Journal of mathematical biology. 2008 Oct;57:557-93.

[16] Isham V. Stochastic models for epidemics. Oxford statistical science series. 2005 Jan 1;33:27.

[17] Ahmad S. Pathogenesis, immunology, and diagnosis of latent Mycobacterium tuberculosis infection. Clin Dev

Immunol. 2011;2011:814943. doi: 10.1155/2011/814943. Epub 2010 Dec 27. PMID: 21234341; PMCID: PMC3017943.

[18] Bäumer D, Lee S, Nicholson G, Davies JL, Parkinson NJ, Murray LM, Gillingwater TH, Ansorge O, Davies KE, Talbot K. Alternative splicing events are a late feature of pathology in a mouse model of spinal muscular atrophy. PLoS genetics. 2008 Dec 18;5(12):e1000773.

[19] Samie A, Makuwa S, Mtshali S, Potgieter N, O Thekisoe et al.. Parasitic infection among HIV/AIDS patients at Bela-Bela clinic, Limpopo province, South Africa with special reference to Cryptosporidium Southeast Asian Journal of Tropical Medicine and Public Health, 2014; 45(4)

[20] Christopher Jackson. Multi-State Markov and Hidden Markov Models in Continuous Time. 2023. Version 1.7.1. L https://github.com/chjackson/msm, https://chjackson.github.io/msm/

[21] Shoko, C., Chikobvu, D. Time-homogeneous Markov process for HIV/AIDS progression under a combination treatment therapy: cohort study, South Africa. *Theor Biol Med Model* **15**, 3 (2018). https://doi.org/10.1186/s12976-017-0075-4

[22] Karaca-Mandic, P., Norton, E. C., & Dowd, B. (2012). Interaction terms in nonlinear models. Health Services Research, 47, 255–274. https://doi.org/10.1111/j.1475-6773.2011.01314.x

[23] Moreno R, Ravasi G, Avedillo P, Lopez R. Tuberculosis and HIV coinfection and related collaborative activities in Latin America the Caribbean. Rev Panam Salud Publica. 2020;44:e43. https://doi.org/10.26633/RPSP.2020.43

[24] Getaneh T, Negesse A, Dessie G, Desta M. The impact of tuberculosis co-infection on virological failure among adults living with HIV in Ethiopia: A systematic review and *meta*-analysis. J Clin Tuberc Other Mycobact Dis. 2022 Mar 4;27:100310. doi: 10.1016/j.jctube.2022.100310. PMID: 35284661; PMCID: PMC8913348.

[25] Shoko C. and Chikobvu D. and Bessong P.O. Effects of Antiretroviral Therapy on CD4+ Cell Count, HIV Viral Load and Death in a South African Cohort: A Modelling Study. Pakistan Journal of Biosciences, 2020; 23: 542-551. **DOI:** 10.3923/pjbs.2020.542.551

[26] Dessie, Z.G., Zewotir, T., Mwambi, H. *et al.* Modelling of viral load dynamics and CD4 cell count progression in an antiretroviral naive cohort: using a joint linear mixed and multistate Markov model. *BMC Infect Dis* **20**, 246 (2020). https://doi.org/10.1186/s12879-020-04972-1.

[27] Matlin S. and Spence N. The Gender Aspects of the HIV/AIDS Pandemic. EGM/HIV-AIDS /2000/OP 1, October 2000. https://www.un.org/womenwatch/daw/csw/hivaids/matlinspence.html

[28] Dessie ZG. Modeling of HIV/AIDS dynamic evolution using non-homogeneous semi-markov process. Springerplus. 2014 Sep 17;3:537. doi: 10.1186/2193-1801-3-537. PMID: 25279328; PMCID: PMC4175685.

[29] World Health Organization. End TB Strategy. WHO [Online]. Geneva:WHO, 2015. [Cited 2018 Nov 21]. Available from: https://www.who.int/tb/post2015_strategy/en/

[30] United Nations. UN General Assembly high-level meeting on TB. World Health Organization - Tuberculosis [Online]. New York: UN, 2018. [Cited 2018 Dec 10]. Available from: https://www.who.int/tb/features_archive/UNGA-adopts-TB-declaration/en/

Appendix

Equilibrium states (Stead states)

Disease free equilibrium

Case1: The disease free equilibrium for our model is given by

$$\bar{E}_0 = \{\bar{T}_4, 0,0, \bar{T}_8, 0, \bar{M}, 0,0,0,0,0\} \quad (12)$$

Equation 12 represents a state in which there is neither HIV nor M. tuberculosis population. Only the populations of CD4 T cells, CD8 T cells and macrophages are present in the system. Thus from equation (1) we have;

$$\frac{dT_4}{dt} = \lambda - \mu T_4 = 0$$

Implying that $\bar{T}_4 = \frac{\lambda}{\mu}$.

From equation (4) we have;

$$\frac{dT_8}{dt} = \gamma - \mu T_8 = 0$$

Implying that $\bar{T}_8 = \frac{\gamma}{\mu}$.

Finally from equation (6) we have

$$\frac{dM}{dt} = \sigma - \mu M - \upsilon M - \theta M = 0$$

This yields $\bar{M} = \frac{\sigma}{\mu}$.

Hence the disease free equilibrium state is

$$\{\bar{T}_4, 0,0, \bar{T}_8, 0, \bar{M}, 0,0,0,0,0\} = \{\frac{\lambda}{\mu}, 0,0, \frac{\gamma}{\mu}, 0, \frac{\sigma}{\mu}, 0,0,0,0,0\}$$

Case 2: HIV infected endemic state is given by;

$$\bar{E}_v = \{\bar{T}_4, \bar{T}_{4v}, \bar{T}_{8v}, \bar{T}_8, 0, \bar{M}, \bar{M}_v, 0,0, \bar{V}, 0\}$$

From equation (1): $\bar{T}_4 = \frac{\lambda}{\mu+\beta\bar{V}}$

From equation (2): $\bar{T}_{4v} = \frac{\beta\bar{V}\bar{T}_4}{k_1\bar{T}_{8v}+N_1\tau_1+\mu}$

From equation (3): $\bar{T}_{8v} = \frac{\rho\gamma}{\mu(\mu+\rho)}$

From equation (4): $\bar{T}_8 = \frac{\gamma}{\mu+\rho}$

From equation (6): $\bar{M} = \frac{\sigma}{\mu+\nu V}$

From equation (7): $\bar{M}_v = \frac{\nu\sigma\mu(\mu+\rho)V}{(\mu+\nu V)(k_2\rho\gamma+\mu^2(\mu+\rho)+N_2\tau_2\mu(\mu+\rho))}$

From equation (8): $\bar{V} = \frac{N_2\tau_2 M_v+N_1\tau_1 T_{4v}}{\mu}$

Case 3: M. tuberculosis infected endemic state is given by

$$\bar{E}_{TB} = \{\bar{T}_4, 0,0, \bar{T}_8, \bar{T}_{8m}, \bar{M}, 0, \bar{M}_m, 0,0, B\}$$

From equation (1): $\bar{T}_4 = \frac{\lambda}{\mu}$

From equation (4): $\bar{T}_8 = \frac{\gamma}{\phi+\mu}$

From equation (5): $\bar{T}_{8m} = \frac{\gamma}{\mu(\mu+\phi)}$

From equation (6): $\bar{M} = \frac{\sigma}{\mu+\theta B}$

From equation (7): $\bar{M}_m = \frac{\mu\theta B(\mu+\phi)}{(k_4\phi\gamma+\mu^2(\mu+\phi)+\mu N_5\alpha_2(\mu+\phi))}$

From equation (11): $B = \frac{N_5\alpha_2\theta\mu(\mu+\phi)}{\mu(k_4\gamma\phi+\mu^2(\mu+\phi)+N_5\alpha_2(\mu+\phi))}$

Case 4: Co-infection equilibrium state

This is a case in which both HIV and M. tuberculosis are present. The co-infection equilibrium state is given by;

$\bar{E}_c = \{\bar{T}_4, \bar{T}_{4v}, \bar{T}_{8v}, \bar{T}_8, \bar{T}_{8m}, \bar{M}, \bar{M}_v, \bar{M}_m, \bar{M}_c, \bar{V}, \bar{B}\}$

From equation (1): $\bar{T}_4 = \frac{\lambda}{\mu+\beta\bar{V}}$

From equation (2): $\bar{T}_{4v} = \frac{\lambda\beta\bar{V}}{(\mu+\beta\bar{V})(k_1\bar{T}_{8v}+N_1\tau_1+\mu)}$

From equation (3): $\bar{T}_{8v} = \frac{\rho\gamma}{\mu(\phi+\rho+\mu)}$

From equation (4): $\bar{T}_8 = \frac{\gamma}{(\phi+\rho+\mu)}$

From equation (5): $\bar{T}_{8m} = \frac{\phi\gamma}{\mu(\phi+\rho+\mu)}$

From equation (6): $\bar{M} = \frac{\sigma}{\mu+\nu+\theta B}$

From equation (7): $\bar{M}_v = \frac{\sigma\upsilon V}{(\mu+\upsilon V+\theta B)(k_2\bar{T}_{8v}+\delta B+N_2\tau_2+\mu)}$

From equation (8): $\bar{M}_m = \frac{\theta\bar{B}\bar{M}}{(\mu+\upsilon\bar{V}+\theta\bar{B})(k_4\bar{T}_{8m}+\mu+\omega\bar{V}\bar{M}_m+N_5\alpha_2}$

From equation (9): $\bar{M}_c = \frac{\delta\bar{B}\bar{M}_v+\omega\bar{V}\bar{M}_m}{N_2\tau_2+N_4\alpha_1+k_2\bar{T}_{8m}+\mu}$

From equation (10): $\bar{V} = \frac{N_2\tau_2\bar{M}_v+N_1\alpha_1\bar{T}_{4v}+N_3\tau_3\bar{M}_c}{\mu}$

From equation (11): $\bar{B} = \frac{N_4\alpha_1\bar{M}_c+N_5\alpha_2\bar{M}_m}{\mu}$

Positivity and boundedness of solutions

Since the system of differential equations represents cell population, then all parameters in our model are non-negative. Thus, it can be shown that, given non-negative initial values, the solutions of the system are non-negative. Consider

$\Omega = \{(\mathrm{T}_4 + \mathrm{T}_{4v} + \mathrm{T}_{8v} + M + \mathrm{M}_v + \mathrm{M}_m + \mathrm{M}_c + \mathrm{T}_8 + \mathrm{T}_{8m} + V + B)\epsilon\mathbb{R}_+^{11}: N < \lambda/\mu\}$

Theorem: For the initial conditions given above, the solution; $\mathrm{T}_4, \mathrm{T}_{4v}, \mathrm{T}_{8v}, M, \mathrm{M}_v, \mathrm{M}_m, \mathrm{M}_c, \mathrm{T}_8, \mathrm{T}_{8m}, V, B$; of the system of differential equations are positive then $t \geq 0$ and the region Ω is positively invariant.

Proof: The rate of change in the total population is given by

$$\frac{dN(t)}{dt} = (\lambda + \gamma + \sigma) - \mu N(t) - (k_1 T_{8v} T_{4v} + \tau_1 T_{4v} + k_2 T_{8v} M_v + k_3 T_{8m} M_c + k_4 T_{8m} M_m)$$

Thus we have;

$\frac{dN(t)}{dt} \leq (\lambda + \gamma + \sigma) - \mu N(t)$,

$\Rightarrow e^{\mu t} \frac{dN(t)}{dt} \leq (\lambda + \gamma + \sigma) e^{\mu t} - \mu N(t) e^{\mu t}$, (multiplying by the integrating factor)

$\Rightarrow e^{\mu t} \frac{dN(t)}{dt} + \mu N(t) e^{\mu t} \leq (\lambda + \gamma + \sigma) e^{\mu t}$,

$\Rightarrow \frac{d\{N(t) e^{\mu t}\}}{dt} \leq (\lambda + \gamma + \sigma) e^{\mu t}$,

$\Rightarrow d\{N(t) e^{\mu t}\} \leq (\lambda + \gamma + \sigma) e^{\mu t} dt$,

$\Rightarrow N(t) e^{\mu t} \leq \frac{(\lambda+\gamma+\sigma)}{\mu} e^{\mu t} + c$,

$\Rightarrow N(t) \leq \frac{(\lambda+\gamma+\sigma)}{\mu} + c e^{-\mu t}$,

$\Rightarrow N(t) \leq \frac{(\lambda+\gamma+\sigma)}{\mu} + \left(N_0 - \frac{(\lambda+\gamma+\sigma)}{\mu}\right) e^{-\mu t}$, (applying the initial condition; $t = 0, N(0) = N_0$)

From Equation (1) we have

$\frac{dT_4}{dt} \geq -\mu T_4 - \beta V T_4$

$T_4(t) \geq T_4(0) e^{\int -(\mu+\beta V) dt}$ Thus T_4 is non-negative for all $t > 0$

From Equation 2 we have:

$\frac{dT_{4v}}{dt} \geq -k_1 T_{8v} T_{4v} - \mu T_{4v}$

$T_{4v}(t) \geq T_{4v}(0) e^{\int -(\mu+k_1 T_{8v}) dt}$ Thus T_{4v} is non-negative for all $t > 0$

From Equation (3) we have

$\frac{dT_{8v}}{dt} \geq -\mu T_{8v}$

$T_{8v}(t) \geq T_{8v}(0) e^{\int -(\mu) dt}$ Thus T_{8v} is non-negative for all $t > 0$

From Equation (4)

$\frac{dT_8}{dt} \geq -\phi T_8 M_m - \rho T_8 T_{4v} - \mu T_8$

$T_8(t) \geq T_8(0) e^{\int -(\phi M_m + \rho T_{4v} + \mu) dt}$ Thus T_8 is non-negative for all $t > 0$

From Equation 5

$\frac{dT_{8m}}{dt} \geq -\mu T_{8m}$

$T_{8m}(t) \geq T_{8m}(0) e^{\int -(\mu) dt}$ Thus T_{8m} is non-negative for all $t > 0$

From Equation (6) we have

$\frac{dM}{dt} \geq -\mu M - vVM - \theta BM$

$M(t) \geq M(0)e^{\int -(\mu+\upsilon+\theta)dt}$ Thus M is non-negative for all $t > 0$

From Equation (7) we have

$\frac{dM_v}{dt} \geq -k_2 T_{8v} M_v - \delta B M_v - \mu M_v$

$M_v(t) \geq M_v(0)e^{\int -(k_2 T_{8v}+\delta B+\mu)dt}$ Thus M_v is non-negative for all $t > 0$

From Equation (8) we have

$\frac{dM_m}{dt} \geq -k_4 T_{8m} M_m - \omega V M_m - \mu M_m$

$M_m(t) \geq M_m(0)e^{\int -(k_4 T_{8m}+\omega V+\mu)dt}$ Thus M_m is non-negative for all $t > 0$

From Equation (9) we have

$\frac{dM_c}{dt} \geq -k_3 T_{8m} M_c - k_5 T_{8v} M_c - \mu M_c$

$M_c(t) \geq M_c(0)e^{\int -(k_3 T_{8m}+k_5 T_{8m}+\mu)dt}$ Thus M_c is non-negative for all $t > 0$

From Equation (10) we have

$\frac{dV}{dt} \geq -\mu V$

$V(t) \geq V(0)e^{\int -(\mu)dt}$ Thus V is non-negative for all $t > 0$

From Equation (11) we have

$\frac{dB}{dt} \geq -\mu B$

$B(t) \geq B(0)e^{\int -(\mu)dt}$ Thus B is non-negative for all $t > 0$